

1 **Quantifying the combined effects of multiple extreme floods on river**
2 **channel geometry and on flood hazards**

3 Mingfu Guan^{1*}, Jonathan L. Carrivick², Nigel G. Wright³, P. Andy Sleight¹, Kate. E.H. Staines⁴

4 ¹ School of Civil Engineering and Water@leeds, University of Leeds, LS2 9JT, Leeds, UK

5 ² School of Geography and Water@leeds, University of Leeds, LS2 9JT, Leeds, UK

6 ³ Faculty of Technology, De Montfort University, LE1 9BH, Leicester, UK

7 ⁴ Edge Analytics Ltd, LS2 9DF, Leeds, UK

8

9 **ABSTRACT**

10 Effects of flood-induced bed elevation and channel geometry changes on flood hazards are largely
11 unexplored, especially in the case of multiple floods from the same site. This study quantified the
12 evolution of river channel and floodplain geometry during a repeated series of hypothetical extreme
13 floods using a 2D full hydro-morphodynamic model (LHMM). These experiments were designed to
14 examine the consequences of channel geometry changes on channel conveyance capacity and
15 subsequent flood dynamics. Our results revealed that extreme floods play an important role in
16 adjusting a river channel to become more efficient for subsequent propagation of floods, and that in-
17 channel scour and sediment re-distribution can greatly improve the conveyance capacity of a channel
18 for subsequent floods. In our hypothetical sequence of floods the response of bed elevation was of
19 net degradation, and sediment transport successively weakened even with floods of the same
20 magnitude. Changes in river channel geometry led to significant impact on flood hydraulics and
21 thereby flood hazards. We found that flood-induced in-channel erosion can disconnect the channel
22 from its floodplain resulting in a reduction of floodwater storage. Thus, the frequency and extent of
23 subsequent overbank flows and floodplain inundation decreased, which reduced downstream flood
24 attenuation and increased downstream flood hazard. In combination and in summary, these results
25 suggest that changes in channel capacity due to extreme floods may drive changes in flood hazard.
26 The assumption of unchanging of river morphology during inundation modelling should therefore be
27 open to question for flood risk management.

* Corresponding author: Dr. Mingfu Guan, Research Fellow, School of Civil Engineering, University of Leeds, UK.
Email:mingfu.guan@hotmail.com

28 *Keywords:* river channel geometry, conveyance capacity, numerical modelling, multiple floods

29 **1. INTRODUCTION**

30 Extreme floods are not contained within a river channel, nor are ever composed entirely of water, but
31 rather include considerable sediment transport. Extreme floods exert significant river
32 geomorphological change and these changes can have an extensive and pervasive geological
33 legacy (Alho et al., 2005; Baynes et al., 2015b; Carling, 2013; Carrivick et al., 2010; Guan et al.,
34 2015b). Whilst extreme floods are by definition infrequent and they occur during a very short period
35 of time, field evidence has shown that hydro-geomorphic responses to floods may affect flood hazard
36 and risk due to changes in channel morphology and to subsequent river hydraulics (Borga et al.,
37 2014; Fewtrell et al., 2011; Lane et al., 2007; Marchi et al., 2009).

38 Types of extreme floods include glacial outburst floods, dam bursts and flash floods due to intense
39 rainfall. The morphological imprint (or adjustment) of river channels to extreme floods can cause
40 short-term and long-term impacts on river hydraulics. Indeed many studies have reported the
41 spatiotemporal morphological response to a single extreme flood and to the effects on flood
42 hydraulics of geomorphological impacts during that flood (Baynes et al., 2015a; Nardi and Rinaldi,
43 2015; Sloan et al., 2001; Staines and Carrivick, 2015). Considering longer-term impacts, Carling
44 (2013) indicated that a repeated series of floods is likely to result in sediment exhaustion effects and
45 that subsequent high-magnitude floods may disrupt much of the sedimentary evidence of earlier
46 floods. Therefore, sediment dynamics and the resultant channel geometry adjustment are more
47 complex during a series of floods than during a single event.

48 Increased flooding frequency and/or magnitude are commonly driven by hydrological changes
49 manifest in initial hydrograph properties, such as an increase in peak water discharge. Recently,
50 some studies have reported that geomorphological changes also play a key role in influencing flood
51 hazards (Lane et al., 2007; Neuhold et al., 2009; Slater et al., 2015; Stover and Montgomery, 2001).
52 For instance, bed aggradation decreases channel capacity and bankfull heights, thereby resulting in
53 a wider regional inundation extent. Conversely, channel incision due to in-channel scour during
54 floods lowers bed elevation and increases conveyance capacity of a channel in flood, so leading to
55 smaller overbank flows. Both scenarios imply changes of flood hazard frequency. Therefore, it is
56 reasonable to suggest that effective flood inundation and hydraulic modelling should consider the

57 sensitivity of flood dynamics to the changes in both hydrological and morphological processes.
58 However, recent research on flood modelling has preferred to assume a static river channel
59 geometry both during flood events and between flood events (Guan et al., 2013; Horritt and Bates,
60 2002; Liang, 2010), and thus ignoring cumulative (long-term) erosion or deposition. Exceptions
61 include the study by (Wong et al., 2014)) who reported that the inclusion of bed elevation changes
62 appeared to alter flood dynamics locally, but that it was not significant for flood inundation, and Slater
63 et al. (2015) who using a large number of field studies and statistical analysis concluded that the
64 changes in channel morphology could lead to significant effects on flood hazard frequency. They also
65 mentioned that morphological effects might be even larger and more widespread than the flow
66 frequency effects.

67 The significance of channel geometry in flood hazard has also been reported by Lane et al. (2007)
68 which explored the effects of channel aggradation due to upstream sediment delivery on inundation
69 extent. Lane and Thorne (2007) suggested that future flood risk should be conditioned not only by
70 changes in conveyance capacity, but also by morphological adjustment in response to changes in
71 river flows and/or upstream sediment supply. In this regard, Neuhold et al. (2009) has incorporated
72 river morphological changes to flood risk assessment, and emphasised that the influence of bed
73 elevation changes on flood hazard is much higher than the influence of discharge input variations.

74 Recent research also verified the significant effects of channel adjustments on hydraulics of flood
75 either by field observation (Rickenmann et al., 2015; Wyzga et al., 2015) or by numerical modelling
76 (Guan et al., 2015b; Li et al., 2014; Staines and Carrivick, 2015). In combination and overall, these
77 studies permit a conceptual hypothesis to be proposed that the influence of sediment transport and
78 subsequent channel changes can be a key driver on flood hazard. Testing this hypothesis requires a
79 detailed study on changes in bed elevation during multiple floods and the effects of that
80 morphological change on subsequent flow hydraulics; particularly on flow capacity and flow
81 conveyance.

82 This study aims to evaluate sediment dynamics within a river channel during a repeated series of
83 extreme floods, and the resultant changes in channel geometry, conveyance capacity of the channel
84 in flood and flood hydraulics. The research questions that this paper poses are:

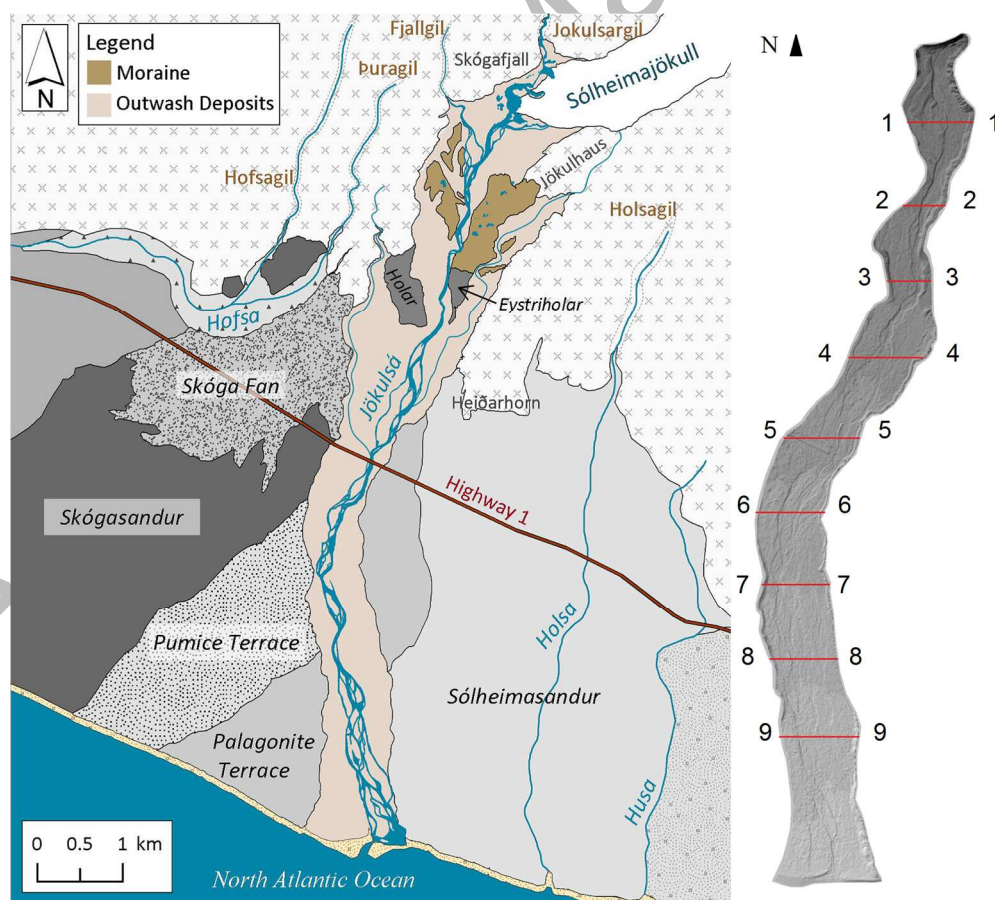
85 (1) How is river channel geometry changed during multiple extreme floods?

86 (2) What effects do river channel geometry changes have on conveyance capacity? and

87 (3) How do changes in river channel geometry influence flood hazards?

88 2. STUDY SITE AND TEST CASE

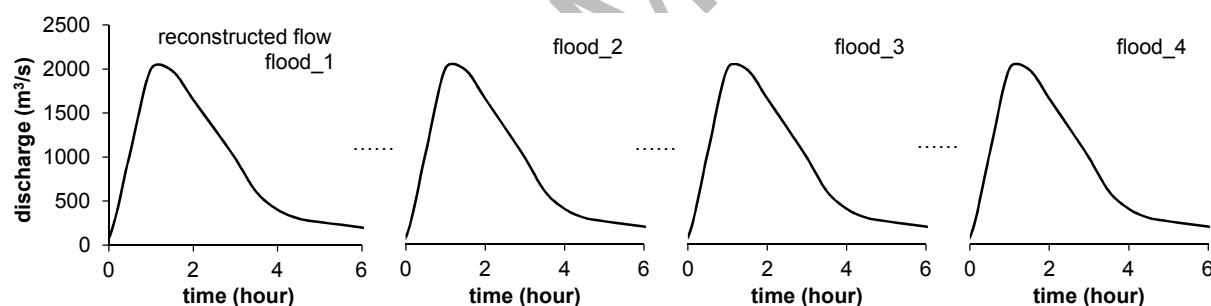
89 A glacial outburst flood that occurred in 1999 at Sólheimajökull in southern Iceland is used as the
 90 study case because of the wealth of morphological (Staines et al., 2014) and hydraulic (Russell et al.,
 91 2010; Staines and Carrivick, 2015) information available for this event. The model performance and
 92 sensitivities have been presented and assessed by Guan et al. (2015b). Building upon this study, the
 93 work here designs and runs a series of experiments in order to elucidate the significance of changes
 94 in river morphology and the necessity of including them for flood hazard analyses. It is worth noting
 95 that Staines and Carrivick (2015) and Guan et al. (2015b) investigated sediment dynamics within the
 96 1999 FLOOD (individual flood) and their geomorphological impacts, but each using different
 97 numerical models. This study differs from both of those by having extended experimental scenarios
 98 to address general concerns that exist in flood hazard assessment.



99
 100 **Figure 1.** (a) Geomorphology of the study river showing the main Jökulsá channel, and (b) digital
 101 elevation model (DEM) of the river channel at 2m × 2m grid cell size resolution

102 The river channel Jökulsá flows from the 8 km long Sólheimajökull outlet glacier that drains from the
 103 Mýrdalsjökull ice cap in the southern volcanic zone of southern Iceland (Figure 1). The river is about
 104 8.7 km in length. Its main flow sources include upstream glacial meltwater and the river Fjallgilsá,
 105 flowing into the Jökulsá approximately 2 km downstream of the glacier snout.

106 The 1999 FLOOD was triggered by subglacial volcanic activity. The flooding process was sudden,
 107 lasted ~ 6 h and had high discharge. The flood burst initially from the western margin of
 108 Sólheimajökull and then flowed into the downstream river channel along with additional meltwater
 109 from the glacier. It was reported by Sigurdsson et al. (2000) that the peak water discharge rose
 110 rapidly to $1700 \text{ m}^3\text{s}^{-1}$ as recorded at the bridge of 4 km downstream ~ 1 hour after the flood initiation.
 111 Peak water discharge at the glacier terminus has been estimated at $4000 \pm 250 \text{ m}^3\text{s}^{-1}$ from the size of
 112 boulders and the velocity required to transport them (Russell et al., 2010). Staines and Carrivick
 113 (2015) pointed out that the peak value $4000 \text{ m}^3\text{s}^{-1}$ was rather high and defined a hydrograph with 40
 114 % of the discharge from the Central Conduit and 60 % from the Western Conduit which was a good-
 115 fit to the observations.



116
 117 **Figure 2.** Inflow hydrograph

118 This study used the input hydrograph provided by Staines and Carrivick (2015) for its first experiment
 119 ('flood_1'). Our subsequent scenarios considered that three more extreme floods with the same peak
 120 discharge occurred in the river channel (named as flood_2, flood_3 and flood_4). Admittedly, flood
 121 sequences in reality differ from each other in terms of hydrograph shape, peak discharge and time. In
 122 this study, we choose same hydrograph shape, peak and time for the experimental flood sequence
 123 because this study strive to: (1) explore sediment transport activities within a same flood magnitude
 124 but a different occurring order, (2) investigate cumulative changes in river morphology during multiple
 125 flood events, and (3) elaborate agglomerate effects of multiple channel adjustments on flood
 126 hazards. Thus, the experiments can provide multiple spatiotemporal viewpoints on morphological

127 changes and impacts during flood sequences. The inflow hydrograph of the simulated scenarios is
128 plotted in Figure 2.

129 To be clear, in this paper we are not specifically focusing on the 1999 FLOOD itself, which has
130 already been explored by (Russell et al., 2010; Staines and Carrivick, 2015; Staines et al., 2014), but
131 rather on quantitatively and qualitatively improving understanding of 'flood memory' and
132 'morphological imprint' during a series of floods. In reality, river morphology may additionally adjust
133 slightly because of human interventions, sediment transport and/or bank erosion caused by perennial
134 flows in channel between each flood. Since the main concern of the study was on the imprint of
135 floods in a riverbed and its flood impact, it was assumed that the slight inter-event changes in river
136 morphology were not significant and neglected. We realise that the exact same scenario will probably
137 not happen repeatedly in the study site. However, widespread and persistent flooding commonly
138 occurs over a short period in reality, such as recent floods across the UK in 2014 and 2015, and this
139 is increasing due to the extreme weather in the context of climate change. Therefore, although this
140 study is running some hypothetical experiments with flood sequences, we consider that the finding
141 from the experiments in this study can profoundly improve the insights into sediment activities within
142 multiple floods and the effects of channel changes on flood hazards, and the finding will be
143 transferable to similar cases suffering from frequent multiple fluvial floods.

144 Pre-flood aerial photographs were taken in August 1996 and post-flood aerial photographs date from
145 August 2001. Both sets were sourced from Landmaelingar Islands (LMI) and orthorectified in Leica
146 Photogrammetry Suite (LPS) with ground control points (GCPs) generated using a Leica GPS500
147 dual phase differential Global Positioning System (dGPS) (Staines et al., 2014). Using the
148 photogrammetry, Staines et al., (2014) built the digital elevation models (DEMs) with 2 m resolution
149 before and after the flood. These pre- and post-flood datasets are a very unusual asset for this kind
150 of modelling study. The 1996 DEM was used as the initial input domain for simulation, and the 2001
151 DEM was used to compare to the simulated bed. DEMs errors and uncertainty were assessed by
152 comparing grid values with the differential Global Positioning System (dGPS) and with a DEM
153 constructed from a 2010 summer LiDAR survey, which is assumed had no errors. The 1999 flood
154 eroded and carried a considerable amount of sediment, causing rapid bed change. However, it is
155 quite challenging to quantify such spatiotemporal river channel adjustment. Therefore, the difference

156 of DEMs (DoD) before (1996 DEM) and after (2001 DEM) the 1999 flood was used to be
 157 approximate quantification of ‘real’ bed changes caused by the flood, although there are some extra
 158 perturbations over the time scale of five years.

159 3. METHODOLOGY

160 3.1 Numerical model - LHMM

161 The hydro-morphodynamic model (LHMM) that has been presented in previous work (Guan et al.,
 162 2014; Guan et al., 2015a; Guan et al., 2015b) was applied in this study and thus is only briefly
 163 described here. LHMM solves fully coupled shallow water equations (SWEs) and sediment transport
 164 model: both bedload and suspended load. Two-dimensional (2D) depth-averaged SWEs are solved
 165 for predicting rapidly varying unsteady flows, and a non-uniform sediment transport model is
 166 developed for bed erosion and deposition. The model considers mass and momentum exchange of
 167 non-cohesive sediment between the bed and the flow, and updates the hydraulic and sediment
 168 quantities per grid cell, per time step. The 2D hydro-morphodynamic model is solved by using a
 169 robust Godunov-type finite volume method.

170 3.1.1 Hydrodynamic model

171 The depth-averaged SWEs with flow-sediment interactions are written in vector form as follows:

$$172 \quad \frac{\partial \mathbf{U}}{\partial t} + \nabla \cdot \mathbf{F} = \mathbf{S}_o + \mathbf{S}_f + \mathbf{S}_{f-b} \quad (1)$$

173 where \mathbf{U} is the vector of conserved variables, \mathbf{F} is the flux vector function, \mathbf{S}_o , \mathbf{S}_f , and \mathbf{S}_{f-b} are the
 174 vector of bed slope term, frictional slope term and flow-bed interaction term, and $\nabla = \vec{i}(\partial/\partial x) +$
 175 $\vec{j}(\partial/\partial y)$ is the gradient operator.

$$176 \quad \mathbf{U} = \begin{pmatrix} \eta \\ hu \\ hv \end{pmatrix}, \quad \mathbf{F} = \begin{pmatrix} h\mathbf{V} \\ hu\mathbf{V} + \frac{1}{2}gh^2\vec{i} \\ hv\mathbf{V} + \frac{1}{2}gh^2\vec{j} \end{pmatrix}, \quad \mathbf{S}_o = \begin{pmatrix} 0 \\ -gh\frac{\partial z_b}{\partial x} \\ -gh\frac{\partial z_b}{\partial y} \end{pmatrix}$$

$$177 \quad \mathbf{S}_f = \begin{pmatrix} 0 \\ -ghS_{fx} \\ -ghS_{fy} \end{pmatrix}, \quad \mathbf{S}_{f-b} = \begin{pmatrix} 0 \\ \frac{\Delta\rho u}{\rho} \frac{\partial z_b}{\partial t} [\alpha(1-p) - C] - \frac{\Delta\rho gh^2}{2\rho} \frac{\partial C}{\partial x} - \mathbf{S}_{ad} \\ \frac{\Delta\rho v}{\rho} \frac{\partial z_b}{\partial t} [\alpha(1-p) - C] - \frac{\Delta\rho gh^2}{2\rho} \frac{\partial C}{\partial y} - \mathbf{S}_{ad} \end{pmatrix} \quad (2)$$

178 where h = flow depth (m); z_b = bed elevation (m); $\eta = h + z_b$ = water surface (m); u, v = the x and y
 179 components of flow velocity (m/s); \mathbf{V} is the velocity vector defined by $\mathbf{V} = u\vec{i} + v\vec{j}$; p = sediment
 180 porosity (dimensionless); C = total volumetric sediment concentration including both bedload and
 181 suspended load (dimensionless); ρ_s, ρ_w = densities of sediment and water respectively (m^3s^{-1});
 182 $\Delta\rho = \rho_s - \rho_w$; ρ = density of flow-sediment mixture (m^3s^{-1}); S_{fx}, S_{fy} are Manning-based frictional slopes in
 183 x and y direction (dimensionless); $\alpha = u_s/u$ = sediment-to-flow velocity ratio (dimensionless) defined by
 184 the equation presented by Greimann et al. (2008); \mathbf{S}_{ad} is the additional term vector related to the
 185 velocity ratio α defined by

$$186 \quad \mathbf{S}_{ad} = \frac{\Delta\rho\mathbf{V}}{\rho} (1 - \alpha) [C\nabla \cdot (h\mathbf{V}) - (h\mathbf{V})\nabla \cdot \mathbf{C}] \quad (3)$$

187 where \mathbf{C} is the sediment concentration vector defined by $\mathbf{C} = C(\vec{i} + \vec{j})$.

188 3.1.2 Sheet flow load

189 Sheet flow load was defined as bedload dominant transport including portion of suspended load
 190 (Pugh and Wilson, 1999; Sumer et al., 1996). Sheet flow has highly concentrated sediment occurs in
 191 a layer near the bed with a thickness of several times sediment grain size. The velocity in this layer is
 192 usually lower than the water velocity, thus the model considers the sediment-to-flow velocity ratio. As
 193 the channel bed was composed of several sediment fractions with different grain sizes, a non-uniform
 194 model was preferable. For each size class, the governing equation (mass-balance) of non-equilibrium
 195 sheet flow was applied following Guan et al. (2014).

$$196 \quad \frac{\partial hS_{bi}}{\partial t} + \frac{\alpha\partial huS_{bi}}{\partial x} + \frac{\alpha\partial hvS_{bi}}{\partial y} = -\frac{\alpha(q_{bi} - F_i q_{b*i})}{L_i} \quad (4)$$

197 where S_{bi} = volumetric bedload concentration of the i th size class; q_{bi} = real sediment transport rate of
 198 the i th fraction; q_{b*i} = sediment transport capacity of the i th fraction; L_i = non-equilibrium adaptation
 199 length of sediment transport of the i th fraction determined by using the equation in Guan et al. (2014);
 200 F_i represents the proportion of i th grain-size fraction in total moving sediment.

201 As suggested by Guan et al. (2014), this study chose the combination of the modified Meyer-Peter &
 202 Müller formula (MPM) (Meyer-Peter and Müller, 1948) and the Smart & Jäggi formula (SJ) (Smart
 203 and Jäggi, 1983) based on the bed slopes to calculate transport capacity.

$$q_{b*i} = \varphi \sqrt{g(\rho_s/\rho_w - 1)d_i^3} \quad (5)$$

$$\varphi = \begin{cases} 8(\theta_i - \theta_{cr,i})^{1.5} & 0 \leq S_o < 0.03 \\ 4 \left(\frac{d_{90}}{d_{30}}\right)^{0.2} \frac{h^{1/6}}{n\sqrt{g}} \min(S_o, 0.2) \theta_i^{0.5} (\theta_i - \theta_{cr,i}) & S_o \geq 0.03 \end{cases}$$

where S_o is bed slope; $\theta_{cr,i}$ is critical dimensionless bed shear stress of i th fraction; θ_i is the dimensionless bed shear stress of i th fraction.

3.1.3 Suspended load transport

Suspended load transport was calculated by solving 2D depth-averaged advection-diffusion equation:

$$\frac{\partial hS_i}{\partial t} + \frac{\partial huS_i}{\partial x} + \frac{\partial hvS_i}{\partial y} = \frac{\partial}{\partial x} \left(\varepsilon_x h \frac{\partial S_i}{\partial x} \right) + \frac{\partial}{\partial y} \left(\varepsilon_y h \frac{\partial S_i}{\partial y} \right) + S_{E,i} - S_{D,i} \quad (6)$$

where S_i = volumetric suspended load concentration of the i th size class; $\varepsilon_x, \varepsilon_y$ = turbulent diffusion coefficients of sediment in the x and y direction; $S_{E,i}$ = entrainment flux of sediment of the i th size class; $S_{D,i}$ = deposition flux of sediment of the i th size class; both fluxes is calculated by

$$S_{D,i} = \omega_{f,i} S_{a,i}, \quad S_{E,i} = F_i \omega_{f,i} S_{ae,i} \quad (7)$$

where $S_{a,i}$ is the near-bed concentration at the reference level which refers to the depth of the sheet flow layer; $S_{ae,i}$ is the near bed equilibrium concentration at the reference level determined by the empirical equation of van Rijn (1984).

3.1.4 Bed level change

Bed elevation was updated based on simulated bed erosion or deposition at each grid, by

$$\frac{\partial z_b}{\partial t} = \frac{1}{1-p} \sum_{i=1}^N \left[\frac{(q_{bi} - F_i q_{b*i})}{L_i} + S_{D,i} - S_{E,i} \right] \quad (8)$$

where N is the number of grain size fractions; the values of the parameters in the right side are calculated according to the equations in previous sections.

3.2 Experimental design

To resolve the research questions, a series of experiments with different scenarios were designed in Table 1. The 1999 FLOOD (R1) was simulated to validate the model performance during real-world

227 events, before then running the experiments. The experiments (R2 – R4) were modelled for
 228 understanding morphological records during multiple flood events. The experiments (R5 – R9) were
 229 designed in order to quantitatively assess the changes in conveyance capacity of the channel and
 230 cumulative effects on flood hazard.

231 **Table 1.** Experimental scenarios design

Runs (R)	Inflow	Bed geometry	Explanation	Purpose
R1	the 1999 FLOOD (flood_1)	original bed	with bed change	model validation
R2	flood_2	adjusted bed by flood_1	with bed change	morphological imprint
R3	flood_3	adjusted bed by flood_2	with bed change	
R4	flood_4	adjusted bed by flood_3	with bed change	
R5	the 1999 FLOOD	original bed	fixed bed	
R6	flood_1	adjusted bed by flood_1	fixed bed	quantification of channel capacity, and flood hazard effects
R7	flood_2	adjusted bed by flood_2	fixed bed	
R8	flood_3	adjusted bed by flood_3	fixed bed	
R9	flood_4	adjusted bed by flood_4	fixed bed	

232
 233 Regarding the model simulations, the river channel was discretised by 1090×288 grids with the grid
 234 size being 8×8 m². The upstream inflow boundary is the hydrograph shown in Figure 2, and the
 235 downstream, left and right boundary are set to be open. For each run, we assumed that Manning's
 236 roughness was not affected by channel adjustment. The Manning-Strickler equation $n = 0.038d_{90}^{1/6}$
 237 was used to estimate the value of Manning's roughness. The depth of the eroded bed is considered
 238 to be unlimited during the flooding. Sediment material in the channel was composed of various grain-
 239 sizes from fine granule to coarse boulder. Three size classes were considered in this study: granules
 240 ($d_{50} = 2.8$ mm), cobbles ($d_{50} = 105$ mm) and boulders ($d_{50} = 400$ mm). It was assumed that the
 241 outburst flood was initially 'clear water'. In-channel erosion and deposition was the main sediment
 242 activity that the flood induced. A variable time step Δt based on a constant Courant–Friedrichs–Lewy
 243 (CFL) number, adapted to local flow conditions, was used to maintain the model stability. The model
 244 (in)sensitivity to some parameters such as mesh size, manning's roughness, parameterisation of
 245 grain-size and choice of sediment transport formulas has been analysed and detailed in Guan et al.
 246 (2015b).

247 4. RESULTS AND DISCUSSION

248 4.1 Morphological response to the 1999 flood

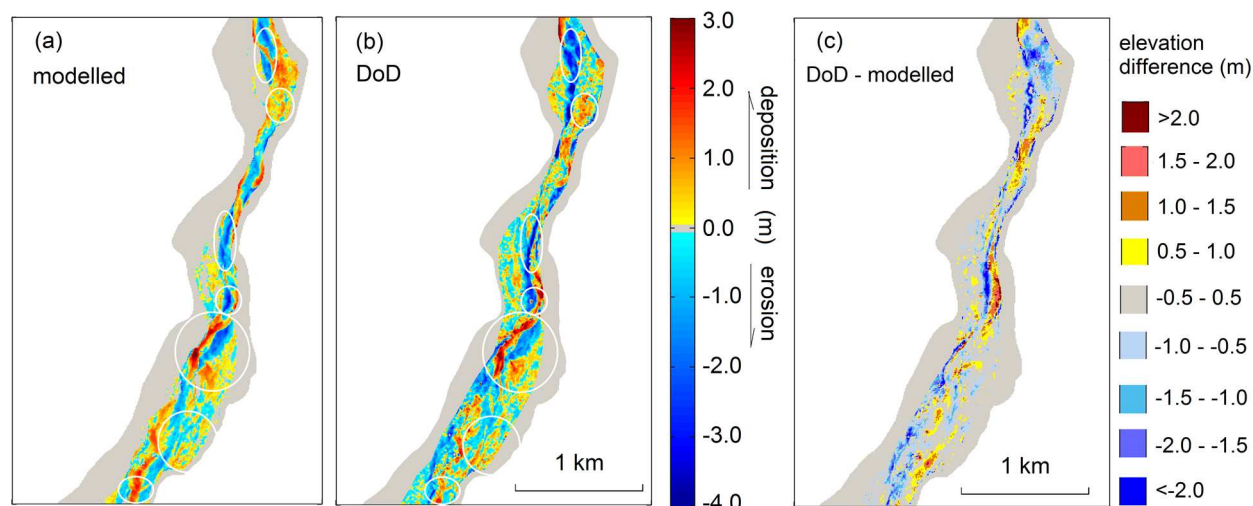
249 Although the 1999 flood has been investigated by some researchers (Russell et al., 2000;
 250 Sigurdsson et al., 2000; Staines et al., 2014), but an exact record and quantification of flood
 251 information has been unattainable. Therefore, in this study we compared our modelled results with
 252 palaeocompetence measurements presented by Staines and Carrivick (2015) and with the slope-
 253 area reconstructions by Russell et al., (2010). The comparison is given in Table 2. It shows that the
 254 differences exist between each other for the hydraulic factors because of the high uncertainty of the
 255 data source. Whilst the modelled arrival time of peak flow to the bridge is about 1 h 13 min, which in
 256 general agrees with the recorded time by Sigurdsson et al. (2000) and with the reconstructions by
 257 Staines (2012).

258 **Table 2.** Comparison of reconstructed hydraulics at the glacier terminus

	Velocity (m^3s^{-1})	Flow Depth (m)	Time to peak in the bridge (h)
Point measurements (Russell et al., 2010)	13 (mean)	7.6	~1 h
Slope-area reconstructions (Russell et al., 2010)	~5 - 7	3.3 – 4.8	N/A
Sigurdsson et al. (2000)	N/A	N/A	~1 h
Modelled results at peak	8.5	3.81	1h 13 min

259 As the DEMs before and after the 1999 flood were reconstructed, the modelled river channel
 260 changes were compared to difference of DEMs (DoD) before (1996 DEM) and after (2001 DEM) the
 261 flood so as to verify the capability of the model in predicting geomorphological changes. The
 262 comparison is demonstrated in Figure 3. It should be clarified that: (1) the time scales of DoD and
 263 modelled changes in riverbed are different; the time interval is ~ 5 years for DoD, while it is only 6
 264 hours for modelled result (Staines and Carrivick, 2015); (2) sediment materials from upstream glacial
 265 areas were likely brought to downstream river, but this was not quantified; (3) the river channel is
 266 complex but its parameterisation for model is in general simplified. Considering a series of
 267 uncertainties, we found from Figure 3 that the modelled channel changes are in general agreement
 268 with the DoD, which is acceptable particularly without any parameter calibrations. We considered the
 269 result is good because both erosion zones and deposition zones were reasonably predicted by the
 270 model and the modelled result shows very similar spatial pattern with DoD. For example, in the seven
 271 highlighted circle zones, the location and magnitude of bed changes are properly simulated. The
 272 uncertainty due to dataset and model parameterisation inevitably leads to some discrepancies. The
 273 measurements show that the riverbed changes in a wider area. The mean differences between the
 274

275 two (Figure 3c) are in a range of (-0.78m – 0.92m), which means only two-boulder diameters
 276 (diameter of a boulder is 0.4 m). Overall, the present model reasonably reconstructs the full
 277 processes of the 1999 flood including inundation and geomorphological changes.

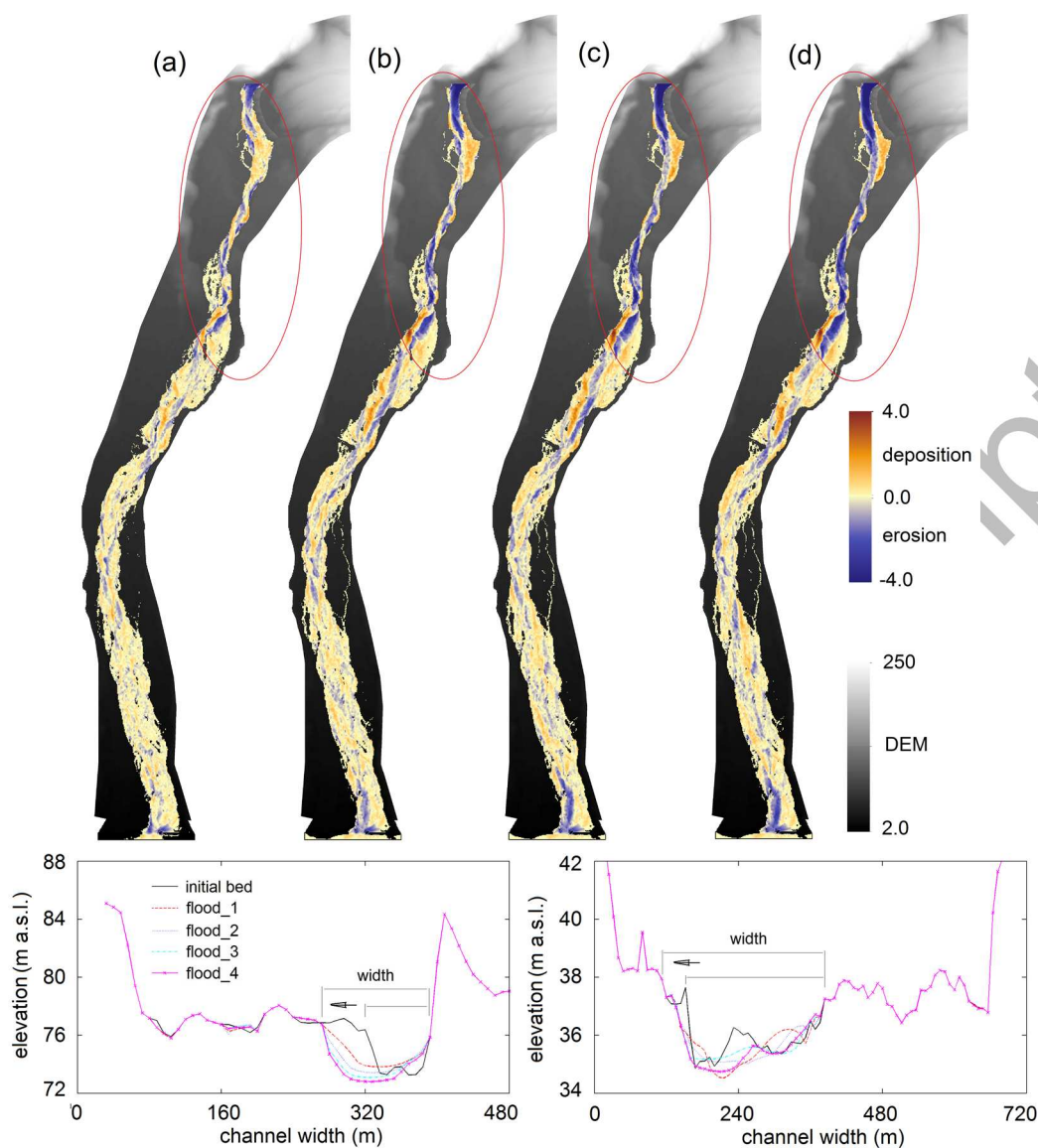


278

279 **Figure 3.** The modelled channel changes, and the DoD of changes in river morphology

280 4.2 Imprint of a series of floods in river morphology

281 We have questioned what the morphological records are due to multiple extreme floods of similar
 282 magnitude. To answer this question, R1 – R4 (Table 1) was performed. Figure 4 shows the modelled
 283 changes in river morphology after flood_1 (R1), flood_2 (R2), flood_3 (R3) and flood_4 (R4), and
 284 channel adjustment to these floods in two cross-sections (CS3 and CS7). Intuitively, it is clear that
 285 more floods aggravate more riverbed erosion. For example, in the circular highlighted area, the main
 286 channel was progressively scoured and more severely with each flood in the sequence. As shown in
 287 the representative cross-sections, the channel incision occurred both vertically and longitudinally so
 288 that the depth and width of the main channel enlarged due to the series of extreme floods. This
 289 channelling has been corroborated in many river cases based on long-term field observation of
 290 morphological activities (e.g.(Nardi and Rinaldi, 2015; Wyzga et al., 2015)). The modelling of this
 291 study evidences that floods generally lead to some imprints in river morphology and the changes will
 292 be exacerbated with more flooding.



293

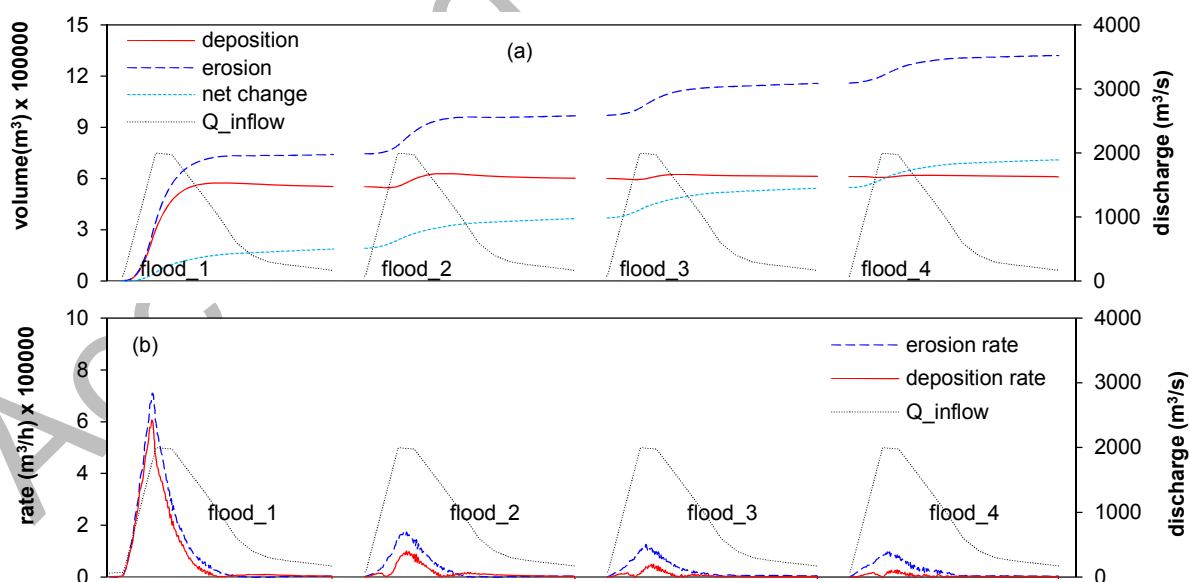
294

295 **Figure 4.** The modelled channel changes after the four successive flood events (a) flood_1, (b) flood_2,
 296 (c) flood_3, and (d) flood_4, and channel adjustment during the four events in (e) CS3 and (f)
 297 CS7. Note: the positive value means deposition, the negative value represents erosion.

298 From a temporal viewpoint, Figure 5 plots the changes of total net erosion, as well as the erosion and
 299 deposition volumes and rates in the whole channel. Surprisingly, we found that even with the same
 300 input hydrograph, successive floods led to significantly different changes in sediment volumes and
 301 rates for each flood. This raised some interesting points about morphological responses to flooding
 302 that previous studies have not detected. The most salient points include that:

- 303 (1) Erosion volume increases with subsequent floods (Figure 5a)
 304 (2) Deposition volume decreases slightly with subsequent floods (Figure 5a).

- 305 (3) Net elevation changes in the river channel imply that successive floods remove sediment
 306 from the bed, i.e. net erosion occurs in the river channel. This commonly occurs in outburst
 307 floods: for example Baynes et al. (2015b) reported that erosion during extreme flood events
 308 dominates the landscape evolution in Iceland.
- 309 (4) Comparing the temporal pattern of erosion and deposition *within* a flood, for successive
 310 events, reveals that high erosion occurs during the peak period of the flood. Interestingly,
 311 deposition also occurs at peak flow because bedload plays an important role in the flooding.
 312 Physically, more bedload is induced into motion from the bed during peak flow and then re-
 313 deposit within an equilibrium length. However, both erosion volume and rate are larger than
 314 the deposition because of the fact that a majority of suspended load and a portion of bedload
 315 were transported within the floodwater.
- 316 (5) The majority of channel adjustments (56 % for erosion and 91 % for deposition) take place
 317 during the first flood.
- 318 (6) Channel changes during subsequent floods become weaker, for bed deposition in particular
 319 (Figure 5b). Deposition volume and rate sharply decrease from flood_1 to flood_4, and it
 320 appears to be stabilising.



321
 322
 323 **Figure 5.** The temporal evolution of: (a) net changes and accumulated erosion and deposition volumes in
 324 the river channel, (b) the erosion and deposition rates

325
 326

327 In combination these six observations signify that a morphological response to extreme floods is to
328 adjust a river channel towards a more efficient propagation of floodwater. Bed response to flood_1 is
329 the most severe, or significant, because of the riverbed is far from an equilibrium state. Once
330 morphological responses, particularly channel straightening, widening and gradient smoothing
331 proceed, bed response becomes more slight even with the same inflow hydraulics.

332 **4.3 Impact of channel adjustment on conveyance capacity**

333 Flood conveyance represents the ability of a river channel to convey floodwater. The capacity of a
334 channel is typically assumed to be stationary in flood risk analysis and channel design engineering.
335 However, there is evidence that the changes in river morphology and sediment supply are leading to
336 increase and/or decrease of conveyance capacity of a river channel and influence flood frequency
337 (Lane et al., 2007; Lane and Thorne, 2007; Slater et al., 2015; Stover and Montgomery, 2001). The
338 previous section of this study has demonstrated the geomorphological activities within the river
339 channel during multiple floods, such as in-channel scour and sediment re-distribution. Yet it is still
340 unclear what impact of channel adjustments on the flood conveyance is. To answer this question, we
341 simulated five scenarios (R5 – R9 in Table 1).

342 Using the flood information modelled by the 2D full hydrodynamic model, we calculated the average
343 stage-discharge rating curves at nine cross-sections along the channel and plotted them in Figure 6.
344 It indicates that flood conveyance capacity increases remarkably at some cross-sections such as
345 CS1, CS2, CS3 and CS7, whilst it changes with relative small magnitude at some cross-sections
346 such as CS4, CS5, CS6, CS8 and CS9. It is clear that changes in flood conveyance are attributed to
347 channel adjustments caused by the floods. Overall, we found that the stage appears to be
348 decreasing for a given discharge under the conditions of considering river morphological changes,
349 despite the fact that the changes in magnitude are different at the nine cross-sections. This means
350 that the extreme floods increase the conveyance capacity of the channel to a certain degree in
351 comparison to the original channel. In general, channel aggradation may lead to a reduction of
352 conveyance capacity of a channel, and conversely, bed degradation should results in an increase of
353 flow capacity (Lane et al., 2007; Slater et al., 2015). It is simple to understand the reason from a
354 viewpoint of cross-section. However, river flows are a dynamic process as a whole, thus its

355 conveyance capacity is not only related to the circumstance of one cross-section, but also affected by
 356 changes in a reach segment.

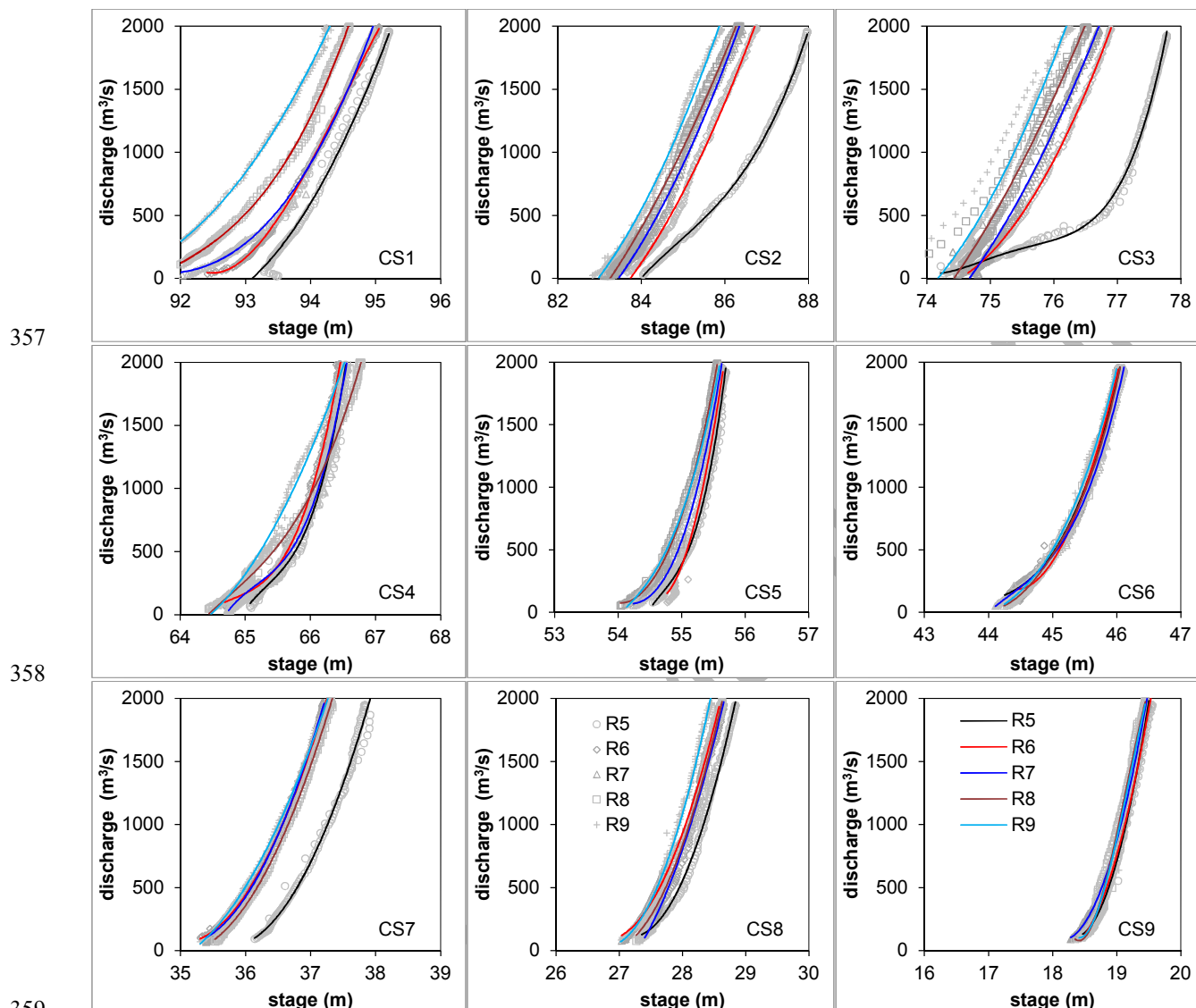
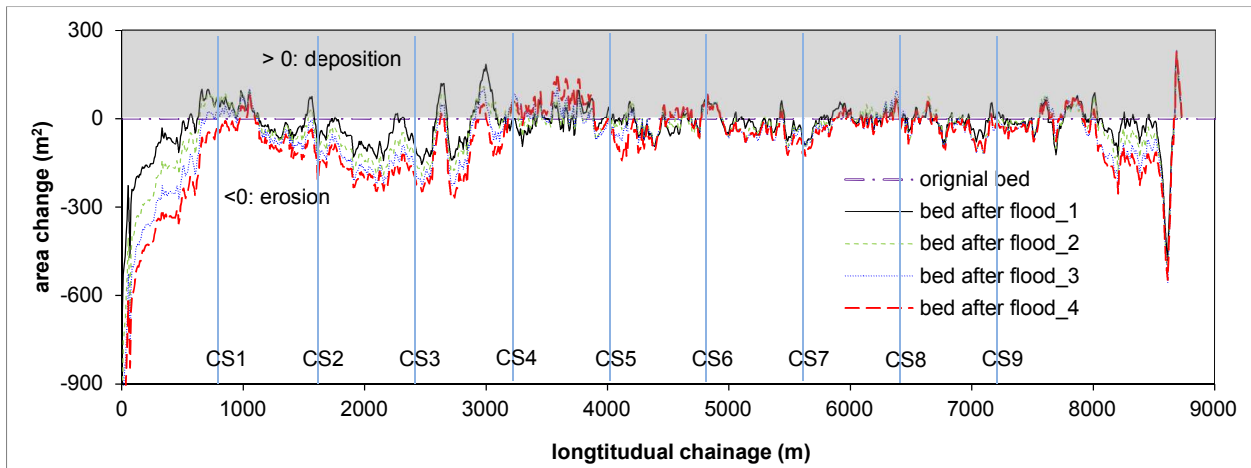


Figure 6. Stage-discharge curves in the nine selected cross-sections during multiple extreme floods

361 We quantified the areas of changes in bed elevations along with the river channel and plotted the
 362 results in Figure 7. It shows that bed erosion dominates in the whole channel (684 in 1090 cross-
 363 sections are eroded after flood_1, and after flood_4 it reaches 818 in 1090). In CS2, CS3 and CS7,
 364 considerable erosion occurs during flood sequence so that the increase in conveyance capacity is
 365 understandable. We can see that in CS1 the water stage for a given discharge is also significantly
 366 decreased from the original bed to the adjusted bed after flood_4, however, the net changes after
 367 flood_1, flood_2 and flood_3 in CS1 are shown to be aggradation, and then it becomes erosion after
 368 flood_4. This finding reveals that bed aggradation in some places does not necessarily cause a

369 decrease of flow capacity of a cross-section; real circumstances of its neighbour areas have equally
 370 important impact on flood stages. The same situation happened in CS6 where channel aggradation
 371 occurs but the flow capacity in CS6 only has slight changes.



372

373

Figure 7. The area of channel changes along with the river channel after each flood

374

375

376

377

378

379

380

381

382

383

384

385

386

387

388

389

390

391

It was found that the overall trend of channel capacity at the nine cross-sections appears to be increasing under the conditions of either degradation or aggradation. As shown in Figure 5a, we may notice that as a whole, the river channel was eroded by multiple extreme floods and the net erosion aggravates along with more flooding. The fact that large account of sediments was washed away from the channel must lead to an increase of conveyance capacity of the whole river segment in flood. Our results suggested that changes in river morphology due to extreme floods is a significant driver of channel conveyance capacity, even though the floods are a short period of time, and that it is a better solution to assess the flow capacity from a reach-scale, not just from a cross-section.

4.4 Effects of changes in riverbed on flood hazard

384

385

386

387

388

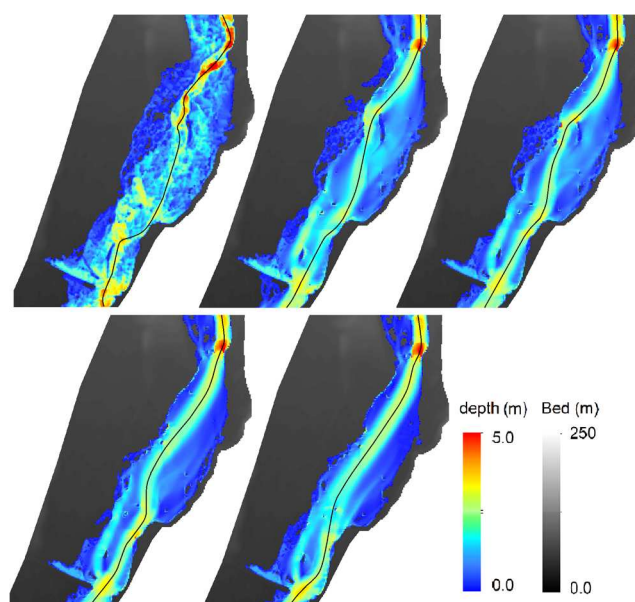
389

390

391

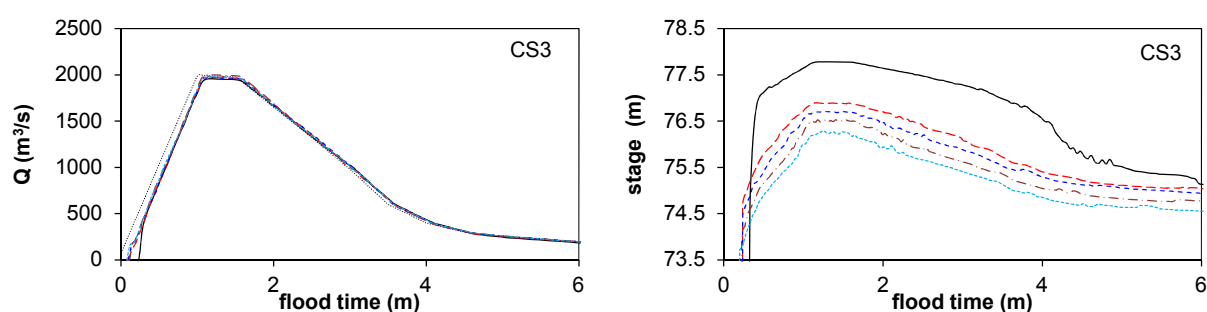
Changes in riverbed play an important role in affecting flood hazards. Therefore, it is crucial to better understand sediment transport and bed elevation changes during floods, especially multiple floods at a same site. For a single extreme flood, Guan et al. (2015b) has given clear evidence of bed changes and significant effects of sediment transport on flood dynamics such as accelerating flood routing, altering flow velocity field and water stages. We next explored the spatial effects of river morphological changes during multiple floods. Figure 8 demonstrates the spatial distribution of modelled water depth at a reach segment when the peak floods over the original channel and the adjusted channels after each flood. It clearly shows that the water depths differ from each other both

392 in terms of distribution and inundation extent. The thalweg line is modified due to changes in channel
 393 morphology after the floods. With more flooding, the main flood pathway appears to be smoother,
 394 more straight and wider. All of these adjustments indicate that river channel is scoured and sediment
 395 is re-distributed towards more efficient to flood propagation.

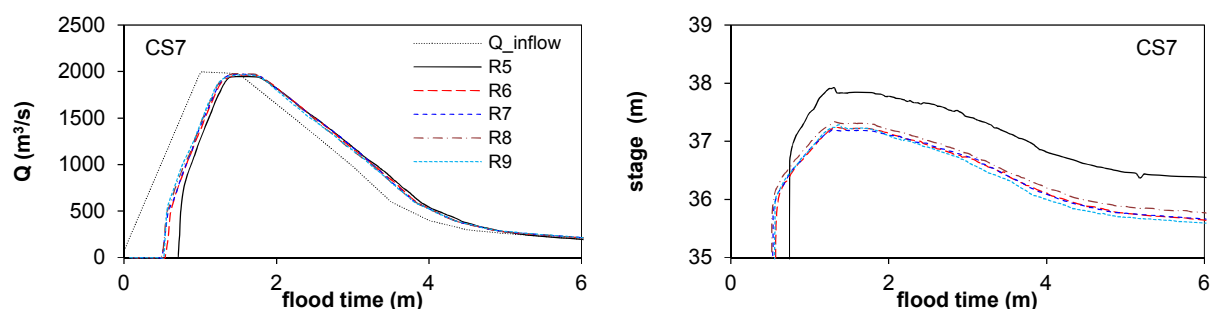


396
 397 **Figure 8.** Water depth at the peak discharge for (a) R5, (b) R6, (c) R7, (d) R8 and (e) R9

398 To further elaborate the impacts of changes in river morphology on flood hazard, we plot the
 399 discharges and the average stage during each flood at CS3 and CS7 in Figure 9. Firstly, it was found
 400 that floods routing through an altered river channel propagated faster than the flood over an
 401 unchanged bed. For example, the difference of the flood arrival time reaches ~12 minutes in CS7. As
 402 noted above, this is attributed to the fact that flooding plays a role in scouring the bed to find its
 403 pathway. However, the latter floods are not accelerated too much even though more flooding occurs
 404 with changes in channel morphology. In alignment with the stage-discharge curves, the averaged
 405 stages of the five scenarios (R5 – R9) at CS3 and CS7 differ from each other significantly. For the
 406 scenario R5, the stage is over 1 m higher than others at CS3, and it is also over 0.6 m at CS7.

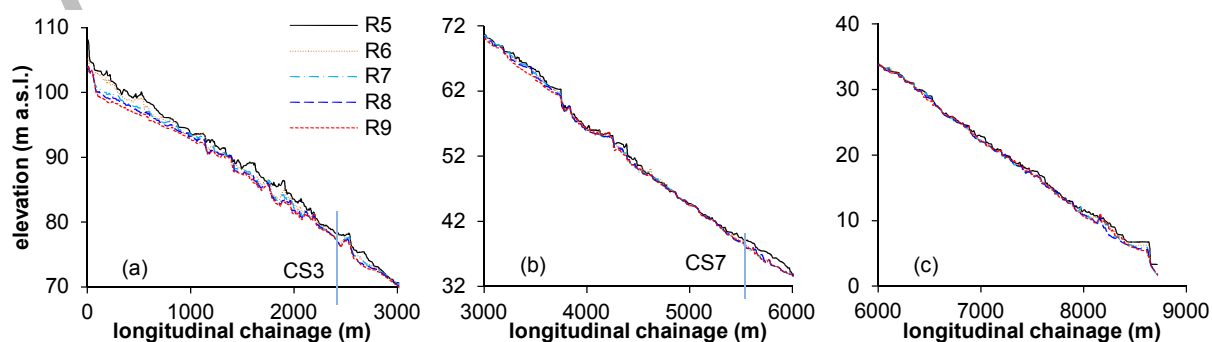


407



408
409 **Figure 9.** Flow discharge and stage over the flooding (R5 – R9) at CS3 and CS7

410 In general, flood stage is considered as an important factor for flood hazard assessment because the
 411 stage level directly decides the inundation extent and the magnitude of overbank flows during a flood.
 412 Figure 10 plots the maximum water stage along with the river channel during the flood over the five
 413 scenarios. It shows that the stage is reduced with more net in-channel erosion throughout the river
 414 channel, particularly at the upstream reach (Figure 10a). At the mid-downstream reach, the stage
 415 decreases in a relatively smaller extent. This coincides with the fact that the bed is scoured more
 416 severely in the upstream reach but slightly in distal reaches as shown in Figure 4. The overall
 417 reduction of maximum water stage will admittedly result in subsequent changes in local and
 418 downstream flood hazard. At CS3 (upstream reach) and CS7 (mid-downstream reach), Figure 11
 419 demonstrates that water stages with a same given discharge ($1965 \text{ m}^3\text{s}^{-1}$) decrease remarkably
 420 because of channel changes during multiple floods. Therefore, this implies that overbank flows to
 421 floodplain (where applicable) must be reduced thereby resulting in a decrease in storage of
 422 floodwater. A comparison of stage-discharge curves between original bed and adjusted bed after a
 423 series of floods (Table 3) indicates that flood-induced in-channel erosion dramatically improved the
 424 conveyance capacity of the channel, thereby resulting dramatic impacts on flood hydraulics. With a
 425 same stage, the discharge at CS3 increases by 1.79 times, and it increases by 1.39 times at CS7. In
 426 other words, flood frequency in the river channel is changed due to changes in river morphology.



427
428 **Figure 10.** Maximum water level for the flood over the five bed scenarios

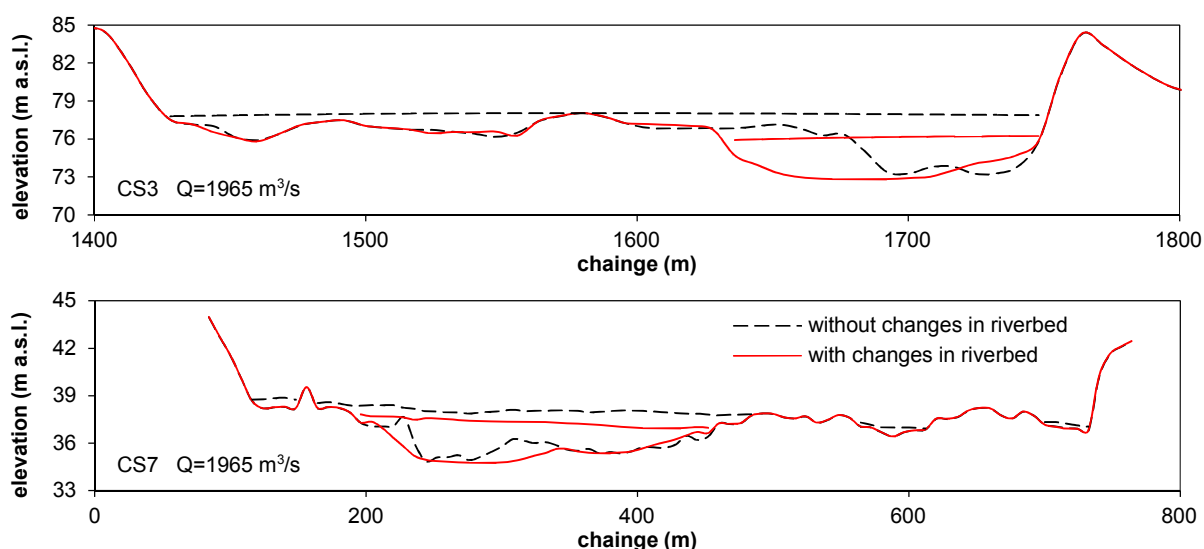


Figure 11. Water stage and bed profile of the original bed and adjusted bed after multiple floods for a given discharge $1965 \text{ m}^3\text{s}^{-1}$

Table 3. Changes in discharge with the same stages at CS3 and CS7 before and after in-channel adjustment due to a series of floods

	Original channel		Adjusted channel due to floods	
	Discharge (m^3s^{-1})	Average stage (m)	Discharge with the same stage (m^3s^{-1})	Increase in discharge
CS3	1965	78.0	3402	$\times 1.73$
CS7	1965	38.0	2734	$\times 1.39$

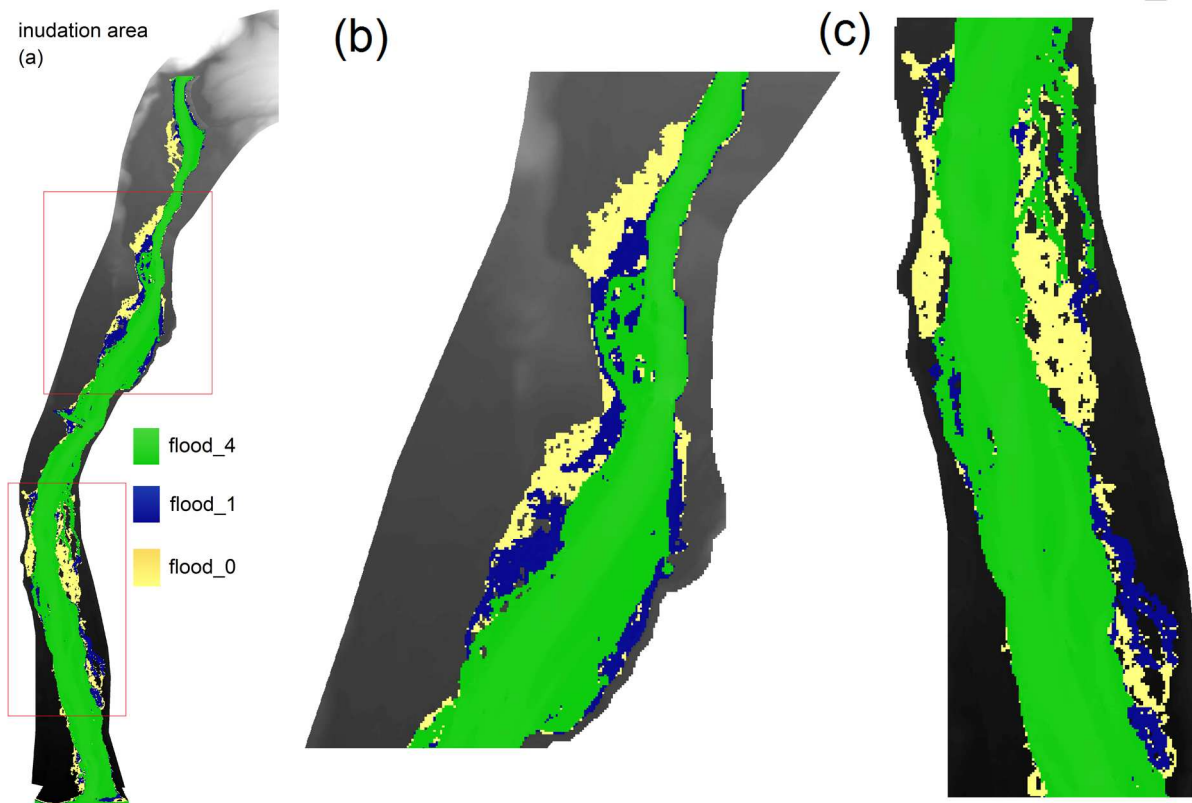
From a spatial point of view, the overlay of flood areas for three scenarios in Figure 12 clearly shows that the in-channel inundation area decreases with a same magnitude flood with agglomerative bed changes (net in-channel erosion), such as the highlighted zone1 and zone2 in Figure 12. Conversely, the net in-channel aggradation can increase flooding inundation extent as reported by Lane et al., (2007). Apparently, flood hazards were significantly affected by channel morphological changes. The effects can be either positive or negative, which is scale- and case-dependent, such as the location of the eroded channel, and floodplain.

The above results raised a number of key understandings in terms of the potential effects of changes in riverbed on flood hazard, including:

- (1) Channel incision due to in-channel scour may lead to disconnect the channel from its floodplain (where applicable) resulting in a reduction of floodwater storage, particularly with further more flooding;

447 (2) The resultant smaller overbank flows and inundation extent implies less flood hazard in the
 448 reach where in-channel erosion severely occurs, because the bankfull water depth
 449 considerably increases for a given discharge.

450 (3) However, at a wider scale, the decrease in overbank flows and floodwater storage must lead
 451 to more floodwater propagate to downstream, i.e. increasing flood hazard frequency in
 452 downstream reaches or areas.



453
 454 **Figure 12.** (a) the inundation extent in the river channel; (b) highlighted zone 1; (c) highlighted zone 2

455 Support for these effects of river channel morphology changes comes from a number of studies that
 456 have investigated the effects of long-term channel incision on flood hydraulics (Shields Jr et al., 2010;
 457 Wohl, 2004; Wyzga et al., 2015). The case here definitely belongs to channel incision due to in-
 458 channel scour caused by extreme floods. Overall, it is emphasised that extreme floods have
 459 consistent effects on in-channel scour. The lowering of channel bed and water stage can greatly
 460 change local and downstream flood hazard that is influenced not only by flow magnitude, but also by
 461 changes in river morphology. This suggests that river channel adjustment caused by flooding can
 462 lead to complex impacts on flood inundation by altering the flow pathway in the channel. At a wider
 463 viewpoint, it is reported that remarkable channel adjustments have taken place in many rivers

464 throughout the world over the last few decades, not only because of multiple flood events, but also in
465 relation to human interventions (e.g. (Abate et al., 2015; Bollati et al., 2014; Campana et al., 2014;
466 Raven et al., 2009; Scorpio et al., 2015)). There is no doubt that these changes in river morphology
467 will lead to significant effects on flow dynamics and inundation during flooding. Effects of both
468 extreme floods and human interventions on river morphology play crucial roles in subsequent flood
469 inundation and thereby flood hazards. This widely emphasises a point raised in the paper: inundation
470 modelling without considering changes in river morphology, as many studies have done, might be
471 open to question for flood hazard assessment.

472 **4.5 Wider applicability**

473 Although this study conducted a set of hypothetical experiments, the resultant findings have wider
474 implications for understanding geomorphological changes during floods and thus for flood hazard
475 analyses. Firstly, extreme floods are a major cause of geomorphological changes in rivers despite
476 the fact that the time scale of individual floods may be very short. Additionally, the changes can be
477 cumulative with a series of big floods. Secondly, given that multiple floods from single sites is very
478 common, the improved understanding of flood-riverbed interactions in this study is applicable
479 worldwide. Thirdly, the significant effects of river morphological changes on flood dynamics found in
480 this study raise a key point for flood risk management: flood hazard is not just from water, but also
481 from flood-driven sediment and/or debris. Any changes in a floodwater pathway (i.e. river channel)
482 can further lead to different propagation time of floods, inundation extent and water stage both locally
483 and downstream. Such consequences of multiple floods and associated geomorphological changes
484 in river channels cannot be neglected, yet frustratingly presently flood risk management tends to be
485 based on assumptions of 'clear water' and a fixed bed. Fourthly, changes in a river channel can
486 typically include localised in-channel scour, aggradation from upland sediment supply, blockage by
487 large debris or large wood, and channel adjustments due to human interventions such as dredging
488 and dumping. Therefore, in future flood hazard assessments should consider both floodwater and its
489 sediment transport and its associated morphological changes. We suggest that the quantified 'flood
490 memory' also provides a reach-scale basis for quantifying the effects of sediment/debris from natural
491 flood management, and river restoration might be necessary to effectively manage flood hazard in a
492 river and its floodplain.

493 **5. CONCLUSIONS**

494 This study explored sediment transport processes during a repeated series of hypothetical extreme
495 floods. An emphasis was placed on the cumulative effects of changes in river morphology on
496 conveyance capacity of a channel in flood and thereby on flood hazards. We have shown that during
497 a series of extreme floods, in-channel erosion occurred more severely in the upper river reach than in
498 the distal reaches (Figure 4). The severe in-channel erosion played an important role in adjusting the
499 river channel to becoming more efficient for flood propagation. Net erosion in the river channel
500 implied that the successive floods consistently removed sediment away from the bed. The majority of
501 channel adjustments took place during the first flood, and channel changes during subsequent floods
502 weakened in intensity and coverage. In other words, the response of the river channel geometry to
503 latter floods approached an equilibrium state based on the imprint of former floods.

504 Our results have shown that both erosion and deposition occurred along with the river channel. This
505 is not surprising but it reinforces the concept that channel capacity increased at some cross-sections
506 and decreased at others. However, overall in-channel scour and sediment re-distribution dramatically
507 increased the conveyance capacity of the river channel in flood in comparison to the original channel.
508 This suggests that it is a better solution to assess the flow capacity from a reach-scale, not just from
509 a cross-section as many studies have done, since flood propagation and transient hydraulics are a
510 fully dynamic process.

511 We have quantified how changes in river channel geometry due to an extreme flood can have a
512 dramatic impact on subsequent flood hydraulics. Firstly, the propagation of floodwater is speeded up,
513 particularly in the channel adjusted by the first flood. Secondly, the thalweg and longitudinal profile of
514 maximum water depth becomes smoother due to changes in channel morphology. Thirdly, water
515 stage for a given discharge decreases as the conveyance capacity increases. Finally, inundation
516 extent within the river channel also decreases because of the lowering of bed elevation and
517 smoothing of the longitudinal profile.

518 These changes in flood hydraulics result in significant impacts on flood hazards locally and at a wider
519 scale. The impacts include a decrease in the frequency and extent of overbank flows and floodplain
520 inundation (where applicable) and at a wider scale this means that the resultant increase in channel
521 capacity and the loss of floodwater storage in its floodplain may reduce downstream flood attenuation

522 and increase flood hazard to downstream reaches and areas. This suggests that special efforts
523 should be made to stabilise upper river reaches for retarding severe bed erosion, and to downstream
524 reaches for flood risk assessment.

525 Overall, this study reinforces the concept that the effects of river channel geometry adjustments on
526 flood hazards are significant and multi-faced. Therefore, properly consideration of changes in river
527 channel geometry during flooding must be made in order to accurately and robustly assess flood risk.
528 We suggest that modelling of floodplain inundation and extreme flooding cannot simply assume river
529 channel consistently unchanged.

530 **ACKNOWLEDGEMENT**

531 MG would like to thank the financial support for his research in the University of Leeds from two cross
532 EPSRC grants: Blue-Green Cities (grant number: EP/K013661/1) and SESAME (grant number:
533 EP/K012770/1). KEHS was funded by a NERC doctoral training grant.

534 **REFERENCES**

- 535 Abate, M. et al., 2015. Morphological changes of Gumara River channel over 50 years, upper Blue Nile
536 basin, Ethiopia. *Journal of Hydrology*, 525: 152-164.
537 DOI:<http://dx.doi.org/10.1016/j.jhydrol.2015.03.044>
- 538 Alho, P., Russell, A.J., Carrivick, J.L., Käyhkö, J., 2005. Reconstruction of the largest Holocene jökulhlaup
539 within Jökulsá á Fjöllum, NE Iceland. *Quaternary Science Reviews*, 24(22): 2319-2334.
540 DOI:10.1016/j.quascirev.2004.11.021
- 541 Baynes, E.R.C., Attal, M., Dugmore, A.J., Kirstein, L.A., Whaler, K.A., 2015a. Catastrophic impact of
542 extreme flood events on the morphology and evolution of the lower Jökulsá á Fjöllum (northeast
543 Iceland) during the Holocene. *Geomorphology*, 250: 422-436.
544 DOI:<http://dx.doi.org/10.1016/j.geomorph.2015.05.009>
- 545 Baynes, E.R.C. et al., 2015b. Erosion during extreme flood events dominates Holocene canyon evolution
546 in northeast Iceland. *Proceedings of the National Academy of Sciences*, 112(8): 2355-2360.
547 DOI:10.1073/pnas.1415443112
- 548 Bollati, I.M., Pellegrini, L., Rinaldi, M., Duci, G., Pelfini, M., 2014. Reach-scale morphological adjustments
549 and stages of channel evolution: The case of the Trebbia River (northern Italy). *Geomorphology*, 221:
550 176-186. DOI:<http://dx.doi.org/10.1016/j.geomorph.2014.06.007>

- 551 Borga, M., Stoffel, M., Marchi, L., Marra, F., Jakob, M., 2014. Hydrogeomorphic response to extreme
552 rainfall in headwater systems: Flash floods and debris flows. *Journal of Hydrology*, 518, Part B: 194-
553 205. DOI:<http://dx.doi.org/10.1016/j.jhydrol.2014.05.022>
- 554 Campana, D., Marchese, E., Theule, J.I., Comiti, F., 2014. Channel degradation and restoration of an
555 Alpine river and related morphological changes. *Geomorphology*, 221: 230-241.
556 DOI:<http://dx.doi.org/10.1016/j.geomorph.2014.06.016>
- 557 Carling, P.A., 2013. Freshwater megaflood sedimentation: What can we learn about generic processes?
558 *Earth-Science Reviews*, 125: 87-113. DOI:<http://dx.doi.org/10.1016/j.earscirev.2013.06.002>
- 559 Carrivick, J.L., Manville, V., Graettinger, A., Cronin, S.J., 2010. Coupled fluid dynamics-sediment transport
560 modelling of a Crater Lake break-out lahar: Mt. Ruapehu, New Zealand. *Journal of Hydrology*, 388(3-
561 4): 399-413. DOI:10.1016/j.jhydrol.2010.05.023
- 562 Fewtrell, T.J., Neal, J.C., Bates, P.D., Harrison, P.J., 2011. Geometric and structural river channel
563 complexity and the prediction of urban inundation. *Hydrological Processes*, 25(20): 3173-3186.
564 DOI:10.1002/hyp.8035
- 565 Greimann, B., Lai, Y., Huang, J.C., 2008. Two-dimensional total sediment load model equations. *Journal*
566 *of Hydraulic Engineering-ASCE*, 134(8): 1142-1146. DOI: [http://dx.doi.org/10.1061/\(ASCE\)0733-
567 9429\(2008\)134:8\(1142\)](http://dx.doi.org/10.1061/(ASCE)0733-9429(2008)134:8(1142))
- 568 Guan, M., Wright, N., Sleigh, P., 2013. A robust 2D shallow water model for solving flow over complex
569 topography using homogenous flux method. *International Journal for Numerical Methods in Fluids*,
570 73(3): 225-249. DOI:10.1002/fld.3795
- 571 Guan, M., Wright, N., Sleigh, P., 2014. 2D Process based morphodynamic model for flooding by
572 noncohesive dyke breach. *Journal of Hydraulic Engineering*, 140(7). DOI:10.1061/(ASCE)HY.1943-
573 7900.0000861
- 574 Guan, M., Wright, N., Sleigh, P., 2015a. Multimode morphodynamic model for sediment-laden flows and
575 geomorphic impacts. *Journal of Hydraulic Engineering*, 141(6). DOI:doi:10.1061/(ASCE)HY.1943-
576 7900.0000997
- 577 Guan, M., Wright, N.G., Sleigh, P.A., Carrivick, J.L., 2015b. Assessment of hydro-morphodynamic
578 modelling and geomorphological impacts of a sediment-charged jökulhlaup, at Sólheimajökull,
579 Iceland. *Journal of Hydrology*, 530: 336-349. DOI:<http://dx.doi.org/10.1016/j.jhydrol.2015.09.062>
- 580 Horritt, M., Bates, P., 2002. Evaluation of 1D and 2D numerical models for predicting river flood
581 inundation. *Journal of Hydrology*, 268(1): 87-99.

- 582 Lane, S.N., Tayefi, V., Reid, S.C., Yu, D., Hardy, R.J., 2007. Interactions between sediment delivery,
583 channel change, climate change and flood risk in a temperate upland environment. *Earth Surface*
584 *Processes and Landforms*, 32(3): 429-446. DOI:10.1002/esp.1404
- 585 Lane, S.N., Thorne, C.R., 2007. River processes. In: Thorne, C.R., Evans, E.P., Penning-Rowell, E.C.
586 (Eds.), *Future flooding and coastal erosion risks*, pp. 82-99. DOI:doi:10.1680/ffacer.34495.0006
- 587 Li, W., van Maren, D.S., Wang, Z.B., de Vriend, H.J., Wu, B., 2014. Peak discharge increase in
588 hyperconcentrated floods. *Advances in Water Resources*, 67(0): 65-77.
589 DOI:http://dx.doi.org/10.1016/j.advwatres.2014.02.007
- 590 Liang, Q.H., 2010. Flood Simulation Using a Well-Balanced Shallow Flow Model. *Journal of Hydraulic*
591 *Engineering-ASCE*, 136(9): 669-675. DOI:10.1061/(asce)hy.1943-7900.0000219
- 592 Marchi, L., Cavalli, M., Sangati, M., Borga, M., 2009. Hydrometeorological controls and erosive response
593 of an extreme alpine debris flow. *Hydrological Processes*, 23(19): 2714-2727. DOI:10.1002/hyp.7362
- 594 Meyer-Peter, E., Müller, R., 1948. *Formulas for bed load transport*, Stockholm, Sweden.
- 595 Nardi, L., Rinaldi, M., 2015. Spatio-temporal patterns of channel changes in response to a major flood
596 event: the case of the Magra River (central-northern Italy). *Earth Surface Processes and Landforms*,
597 40(3): 326-339. DOI:10.1002/esp.3636
- 598 Neuhold, C., Stanzel, P., Nachtnebel, H.P., 2009. Incorporating river morphological changes to flood risk
599 assessment: uncertainties, methodology and application. *Nat. Hazards Earth Syst. Sci.*, 9(3): 789-799.
600 DOI:10.5194/nhess-9-789-2009
- 601 Pugh, F.J., Wilson, K.C., 1999. Velocity and concentration distributions in sheet flow above plane beds.
602 *Journal of Hydraulic Engineering-ASCE*, 125(2): 117-125. DOI:10.1061/(asce)0733-
603 9429(1999)125:2(117)
- 604 Raven, E.K., Lane, S.N., Ferguson, R.I., Bracken, L.J., 2009. The spatial and temporal patterns of
605 aggradation in a temperate, upland, gravel-bed river. *Earth Surface Processes and Landforms*, 34(9):
606 1181-1197. DOI:10.1002/esp.1783
- 607 Rickenmann, D., Badoux, A., Hunzinger, L., 2015. Significance of sediment transport processes during
608 piedmont floods: the 2005 flood events in Switzerland. *Earth Surface Processes and Landforms*: n/a-
609 n/a. DOI:10.1002/esp.3835
- 610 Russell, A.J., Tweed, F.S., Knudsen, Ó., 2000. Flash flood at Sólheimajökull heralds the reawakening of
611 an Icelandic subglacial volcano. *Geology Today*, 16(3): 102-106. DOI:10.1046/j.1365-
612 2451.2000.00005.x

- 613 Russell, A.J. et al., 2010. An unusual jökulhlaup resulting from subglacial volcanism, Sólheimajökull,
614 Iceland. Quaternary Science Reviews, 29(11–12): 1363-1381.
615 DOI:<http://dx.doi.org/10.1016/j.quascirev.2010.02.023>
- 616 Scorpio, V. et al., 2015. River channel adjustments in Southern Italy over the past 150 years and
617 implications for channel recovery. Geomorphology, 251: 77-90.
618 DOI:<http://dx.doi.org/10.1016/j.geomorph.2015.07.008>
- 619 Shields Jr, F.D., Lizotte Jr, R.E., Knight, S.S., Cooper, C.M., Wilcox, D., 2010. The stream channel
620 incision syndrome and water quality. Ecological Engineering, 36(1): 78-90.
621 DOI:<http://dx.doi.org/10.1016/j.ecoleng.2009.09.014>
- 622 Sigurdsson, O., Zóphóníasson, S., Ísleifsson, E., 2000. Jökulhlaup úr Sólheimajökull 18. júlí 1999. , 49, .
623 Jökull, 49: 75-81.
- 624 Slater, L.J., Singer, M.B., Kirchner, J.W., 2015. Hydrologic versus geomorphic drivers of trends in flood
625 hazard. Geophysical Research Letters, 42(2): 2014GL062482. DOI:10.1002/2014GL062482
- 626 Sloan, J., Miller, J.R., Lancaster, N., 2001. Response and recovery of the Eel River, California, and its
627 tributaries to floods in 1955, 1964, and 1997. Geomorphology, 36(3–4): 129-154.
628 DOI:[http://dx.doi.org/10.1016/S0169-555X\(00\)00037-4](http://dx.doi.org/10.1016/S0169-555X(00)00037-4)
- 629 Smart, G., Jäggi, M., 1983. Sediment transport on steep slopes. Mitteilung. 64. Versuchsanstalt für
630 Wasserbau, Hydrologie und Glaziologie, ETH Zurich, Zurich.
- 631 Staines, K.E.H., 2012. Quantifying Landscape Change in a Jökulhlaup-prone Proglacial System
632 Sólheimajökull, Southern Iceland, University of Leeds, Leeds, UK, 224 pp.
- 633 Staines, K.E.H., Carrivick, J.L., 2015. Geomorphological impact and morphodynamic effects on flow
634 conveyance of the 1999 jökulhlaup at sólheimajökull, Iceland. Earth Surface Processes and
635 Landforms: n/a-n/a. DOI:10.1002/esp.3750
- 636 Staines, K.E.H. et al., 2014. A multi-dimensional analysis of pro-glacial landscape change at
637 Sólheimajökull, southern Iceland. Earth Surface Processes and Landforms: n/a-n/a.
638 DOI:10.1002/esp.3662
- 639 Stover, S.C., Montgomery, D.R., 2001. Channel change and flooding, Skokomish River, Washington.
640 Journal of Hydrology, 243(3–4): 272-286. DOI:[http://dx.doi.org/10.1016/S0022-1694\(00\)00421-2](http://dx.doi.org/10.1016/S0022-1694(00)00421-2)
- 641 Sumer, B.M., Kozakiewicz, A., Fredsoe, J., Deigaard, R., 1996. Velocity and concentration profiles in
642 sheet-flow layer of movable bed. Journal of Hydraulic Engineering-ASCE, 122(10): 549-558.
643 DOI:[http://dx.doi.org/10.1061/\(ASCE\)0733-9429\(1996\)122:10\(549\)](http://dx.doi.org/10.1061/(ASCE)0733-9429(1996)122:10(549))

- 644 van Rijn, L.C., 1984. Sediment transport part II, suspended load transport. Journal of Hydraulic
645 Engineering-ASCE, 110 (11): 1613–1641. DOI:[http://dx.doi.org/10.1061/\(ASCE\)0733-](http://dx.doi.org/10.1061/(ASCE)0733-9429(1984)110:11(1613))
646 9429(1984)110:11(1613)
- 647 Wohl, E.E., 2004. Disconnected Rivers: Linking Rivers to Landscapes. Yale University Press.
- 648 Wong, J.S., Freer, J.E., Bates, P.D., Sear, D.A., Stephens, E.M., 2014. Sensitivity of a hydraulic model to
649 channel erosion uncertainty during extreme flooding. Hydrological Processes. DOI:10.1002/hyp.10148
- 650 Wyżga, B., Zawiejska, J., Radecki-Pawlik, A., 2015. Impact of channel incision on the hydraulics of flood
651 flows: Examples from Polish Carpathian rivers. Geomorphology.
652 DOI:<http://dx.doi.org/10.1016/j.geomorph.2015.05.017>
- 653